I&EC research
Industrial & Engineering Chemistry Research

Open Access
This article is licensed under CC-BY 4.0

pubs.acs.org/IECR
Article

Effect of Temperature on Aqueous Two-Phase Systems Based on Acetonitrile and Protic Ionic Liquids: Phase Diagram and Partitioning of Commercial Biomolecules Present in Clove Oil

Jarlon Conceição da Costa, Isabela Conceição Sales, Bruna Vida da Ressureição, Luciano Morais Lião, Gerlon de Almeida Ribeiro Oliveira, Álvaro Silva Lima, Luiz Mário N Góis, and Silvana Mattedi*

Cite This: *Ind. Eng. Chem. Res.* 2025, 64, 5602−5616
Read Online

ACCESS | Metrics & More | Article Recommendations | Supporting Information

ABSTRACT: Recently, ionic liquids (ILs) have been applied in extraction and separation processes due to their chemical and physical properties arising from the cations and anions that form these liquids. In aqueous two-phase systems (ATPSs), ILs can be used as phase formers and assist in the separation and purification processes of biomolecules, such as phenolics and terpenes present in clove oil. In this work, the effect of temperature (288.2, 298.2, and 308.2 K) and the alkyl chain size of protic ionic liquid (PIL) anion in ATPSs based on PIL + acetonitrile (ACN) + water at 101.2 kPa is evaluated. The NRTL and UNIQUAC models were used to predict the LLE data. The increase in the temperature and the alkyl chain compressed the biphasic region of the phase diagram. In the proposed systems, partitioning data were obtained for commercial biomolecules present in clove oil (eugenol, eugenyl acetate, and α-humulene). Phenolics (eugenol and eugenyl acetate) were partitioned to the PIL-rich phase. In contrast, α-humulene (terpene) was partitioned into the ACN-rich phase. It was observed that increasing temperature increases or maintains almost constant the recovery of biomolecules in the bottom phase (R_B) from similar tie-line length (TLL). Additionally, eugenol and eugenyl acetate can be partially isolated (selectivity: S = 2.17) at 298.2 K. Finally, the highest values achieved for bottom phase recoveries for the target biomolecules were achieved using ATPS formed by [2HEA][Bu] + ACN + water (TLL ≈ 53 and 57.57 < R_B < 93.54). PILs can be used as a salting-out agent to form biphasic phase systems with acetonitrile and separate biomolecules where reasonable recovery rates were verified.

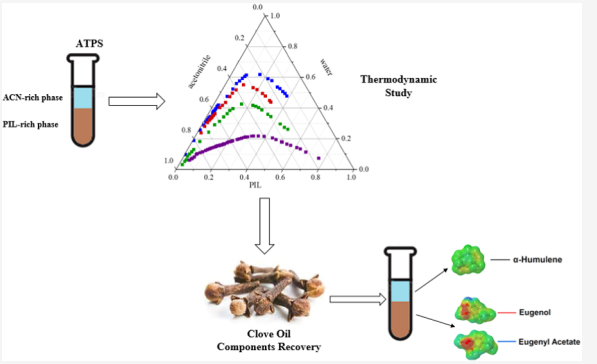

Downloaded via 177.86.74.246 on September 29, 2025 at 11:27:49 (UTC).
See https://pubs.acs.org/sharingguidelines for options on how to legitimately share published articles.

1. INTRODUCTION

Recent studies show new methods and applications of processes in the separation and purification processes of biomolecules. Aqueous two-phase systems (ATPS) and liquid−liquid equilibrium (LLE) improve the understanding of biomolecule separation data (phenolic compounds, terpenes, and alkaloids), especially in systems based on protic ionic liquids (PILs). The scientific community has been suggesting using ionic liquids (ILs) to form ATPS for the extraction and separation of bioactive components present in essential oils, natural products, and biomass, enabling the replacement of traditional solvents, varying processes, and promoting sustainability.[1−6]

The clove essential oil is composed of a complex mixture of compounds with low molecular weights possessing volatile compounds such as monoterpenes, sesquiterpenes, and phenolic hydrocarbons. Due to its antioxidant, antimicrobial, and anti-inflammatory potential, this oil is primarily used as an additive in food and medicinal products.[7] As with other essential oils, it is also used to produce cosmetic and hygiene fragrances.[8] Among the components in clove oil, the most relevant are eugenol, α-humulene, α caryophyllene, eugenyl acetate, and minor quantities of carvacrol. β-caryphene and α-farnesene are also present.[9] Different techniques have been proposed to fractionate clove oil, such as micellar electrokinetic chromatography and solvent extraction, including acetonitrile−water.[10]

Recently, ATPS formed by acetonitrile, water, and ILs have been proposed for biomolecule separation.[11−13] To apply this system for purification processes, liquid−liquid equilibria should be investigated to develop more efficient methods for separating components of interest and adjusting to better operational conditions as usual for other liquid−liquid systems.[9] Some factors, such as pH, molecular weight,

Received: August 23, 2024
Revised: February 7, 2025
Accepted: February 10, 2025
Published: March 3, 2025

© 2025 The Authors. Published by American Chemical Society

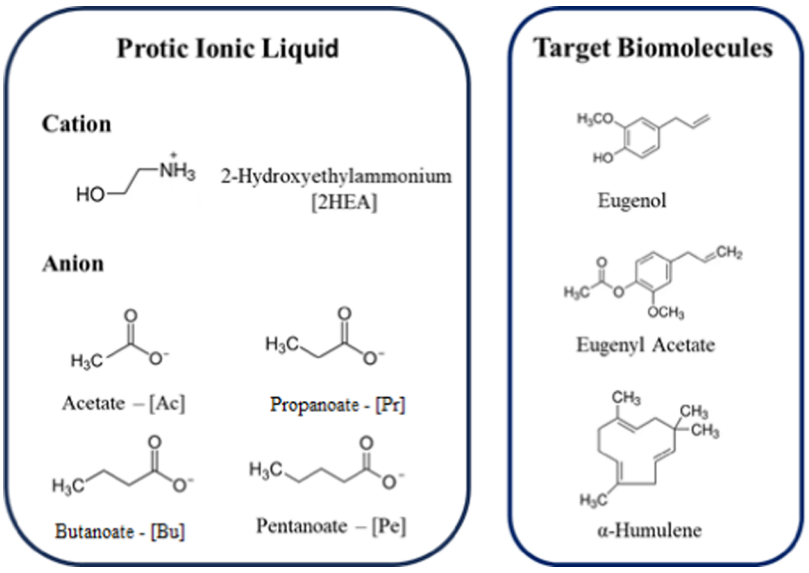

Figure 1. Chemical structure of PIL precursors and target biomolecules

concentration, and temperature, influence the partitioning of biomolecules. The temperature affects the composition of phases and the partition through viscosity and density.[14]

The spontaneous formation of an ATPS occurs when two compounds are mixed in water at a particular critical thermodynamic, such as a specific range of temperature, pressure, and composition of constituents.[2,3] They are usually formed by polymer−polymer, salt−salt, or polymer−salt complexes. Physicochemical and thermodynamic properties between the phases of the system lead to a different distribution of the biomolecule of interest in the phases.[4] ATPSs are applied in biomolecular separation and purification processes, such as phenolic compounds, enzymes, alkaloids, proteins, lignocellulosic biomass pretreatment, and mineral extraction, used on analytical and industrial scales.[11−13]

Being one of the components in the formation of ATPS, ILs are low melting point organic salts, usually liquid at temperatures below 100 °C. These properties generally lead to low volatility, flammability, and a wide liquid temperature range.[11,13] Moreover, ILs could be designed for specific purposes by preselecting diverse combinations of cations and anions, therefore being called design solvents.[15] Due to these features, ILs have been used in different applications in chemical synthesis, biocatalytic transformation, hydrotropes for enhancing the solubility of compounds in aqueous solutions, electrochemistry, analytical, separation and extraction processes[5,15,16] and as an alternative solvent for separation, including purification of biocompounds using ATPS.[17] However, due to the numerous possible combinations of anions and cations, relatively few data are available for thermodynamic properties and phase equilibria.[18]

Ionic liquids are classified based on the groups present, such as protic and aprotic ionic liquids. Aprotic ILs (AILs) comprise the largest class of ILs and are synthesized by the irreversible alkylation mechanism of a nucleophile with an electrophile. Compared to PILs, they are also adjustable and have several applications, including purification of biomolecules.[19] Protic ionic liquids (PILs) are directly produced through the neutralization process of a Brønsted acid and a Brønsted base, forming an ionic liquid through proton transfer in a one-step synthesis.[20] In this work, PILs based on 2-hydroxyethylamine and short-chain carboxylic acid present low toxicity at various trophic levels and their potential biodegradability.[21] Low-toxicity systems are generally targeted for biomolecule purification, such as recent studies in thermoreversible ATPS.[22] These liquids may present disadvantages such as reversible reaction, depending on the strength of the acid and the base used, stability depending on the pH value of the system, and a decrease in ionic conductivity.[23]

Concerning the use of AILs and PILs, studies reveal the possibility of using AILs to recover antioxidant compounds (including eugenol) and fractionation of essential oils.[1,24] However, there are no studies by building phase diagrams (including binodal curves, tie lines, and partition) that demonstrate the use of ATPS based on PILs and acetonitrile for the separation of the components of essential oils, such as clove oil and their biomolecules, for example, eugenol, eugenyl acetate, and α-humulene. Acetonitrile (ACN) was chosen because it is a solvent used to extract compounds of industrial interest for applications in cosmetics, pharmaceuticals, and essential oils. It is very significant in the extraction of biomolecules. This solvent enables yields similar or superior to those of traditional solvents. Acetonitrile is entirely soluble in water; however, it forms a biphasic system with water in the presence of the same solutes as carbohydrates or ionic liquids.[25]

The main goal of this work is to construct phase diagrams formed by ACN + PIL (cation: 2-hydroxyethylammonium—2HEA; and anions: acetate, propanoate, butanoate, or pentanoate) at three different temperatures (288.2, 298.2, and 308.2 K) under atmospheric pressure (101.3 kPa), investigate the correlation of liquid−liquid equilibrium data with NRTL (non-random two-liquid) and UNIQUAC (Universal Quasichemical) models, and apply the ATPSs formed in the partitioning of biomolecules commonly found in clove oil such as eugenol, eugenyl acetate, and α-humulene.

2. MATERIALS AND METHODS

2.1. Material. PILs were synthesized using 2-hydroxyethylamine—[2HEA] (purity = 99%) and different organic acids such as acetic acid (purity ≥99%), propionic acid (purity ≥99%), butanoic acid (purity ≥99%), and pentanoic acid

https://doi.org/10.1021/acs.iecr.4c03157
Ind. Eng. Chem. Res. 2025, 64, 5602−5616

(purity ≥99%). The phase diagrams were built using PIL and acetonitrile (purity ≥99.9%). The commercial biomolecules from clove oil, such as eugenol (purity = 99%), eugenyl acetate (purity ≥98%), and α-humulene (purity ≥96%) were used. Figure 1 depicts the chemical structure of the compounds, and Table 1 shows their characteristics. Ultrapure water that was

Table 1. Chemical Characteristics of the Compounds Used in This Work

compounds	molar mass (g mol^{-1})	CAS number	supplier
2-hydroxyethylamine	61.08	141−43−5	Sigma-Aldrich
acetic acid	60.05	64−19−7	Sigma-Aldrich
propionic acid	74.09	79−09−4	Sigma-Aldrich
butanoic acid	88.11	107−92−6	Sigma-Aldrich
pentanoic acid	102.13	109−52−4	Sigma-Aldrich
acetonitrile	41.05	75−05−8	Merck
eugenol	164.20	97−53−0	Sigma-Aldrich
eugenyl acetate	206.24	93−28−7	Sigma-Aldrich
α-humulene	204.35	6753−98−6	Sigma-Aldrich

double-distilled, passed through a reverse osmosis system, and further purified by Milli-Q Plus 185 water purification apparatus (Millipore, Bedford, MA) was used in all experiments.

2.2. PIL Synthesis. Five PILs were synthesized by a simple acid−base neutralization reaction described by Álvarez et al.[26] The 2-hydroxyethylamine was placed in a three-necked flask of glass equipped with a reflux condenser. The organic acid was added dropwise to the flask at 298.2 K under stirring with a magnetic bar. The synthesis was carried out in an inert atmosphere using nitrogen gas. The reaction occurs stoichiometrically in a 1:1 molar ratio and is exothermic. 1 mol of each reactant was used in each reaction. The reaction is complete when the heat release ceases. After the reaction was finished, the liquids were placed under constant agitation in a rotary evaporator under a moderate vacuum (50 kPa) at 318.2 K for 144 h and further under a high vacuum (20 Pa) at 323.2 for 48 h to eliminate residual reactants and excess water excess. NMR confirms the formation and purity of the PILs. The water content was measured using a Mettler Toledo V20 volumetric Karl Fischer titrator (Columbus, Ohio) before each experiment and was considered in the calculation. The synthesized PIL were 2-hidroxylethylammonium acetate, [2HEA][Ac], 2-hidroxylethylammonium propanoate, [2HEA][Pr], 2-hidroxylethylammonium butanoate, [2HEA][Bu], and 2-hidroxylethylammonium pentanoate—[2HEA][Pe].

NMR evaluated the PIL's purity. The NMR spectra were acquired at 293.2 K on a Bruker Avance III 500 spectrometer operating at 11.75 T (500 MHz for ^{1}H). Approximately 30.00 mg of the samples and 470 μL of D_2O were added into 2 mL centrifuge tubes (yielding 155 to 495 mmol·L^{-1} solutions). After being stirred until complete dissolution, the solutions were transferred to 5 mm NMR tubes. To quantify the ionic liquid content in the samples, maleic acid was used as an external standard in five independently prepared solutions in a concentration range of 95 to 578 mmol·L^{-1}. The probe was properly tuned and matched. The magnetic field was optimized (shimming) before each acquisition. The acquisition parameters were 4 and 200 scans (NS), 64 and 32,000 data points (TD), spectral windows (SWs) of 20 and 237 ppm, and acquisition times (AQs) of 1.65 and 1.1 s for ^{1}H and ^{13}C, respectively. A relaxation delay of 2.0 s was used for ^{13}C. For ^{1}H, this delay was set at 60 s for the maleic acid standard and varied from 20 to 40 s for the samples to achieve virtually complete longitudinal relaxation. The pulse length was manually calibrated to optimal 90° excitation, and the acquisitions started after 5 min of temperature stabilization at 20 °C. Each sample was analyzed in triplicate. As an internal reference, all ^{1}H NMR chemical shifts are given in δ (ppm) related to the TMSP-d_4 signal at δ 0.00. The spectra were acquired, processed, and analyzed by using Bruker TopSpin software. NMR signals that did not overlap with impurities were chosen for quantification. The assessment of peak shape and variations in peak areas about the stoichiometry of the molecule detected impurity overlap. The signal-to-noise ratio was always higher than 2000 for the signals used in the quantification.

2.3. Phase Diagrams. Solubility data for the ternary mixture were determined using the cloud point method reported by Kaul.[27] The transition point between the homogeneous and heterogeneous zones was determined visually. The binodal curves were performed for three temperatures: 288.2, 298.2, and 308.2 K, controlled by a water jacket connected to a thermostatic bath. The experimental data were gravimetrically determined using an analytical balance (Shimadzu AX200, Kyoto-Japan). The measurement uncertainty was ±0.1 K for temperature and ±0.001 g for mass.

Briefly, ACN aqueous solution (80 wt %) was added dropwise to PILs aqueous solution (60−80 wt %) until the visual detection of a turbidity (biphasic region). Afterward, water was added dropwise into the system until a clear, limpid solution (monophasic region) was obtained. The procedure was repeated several times under constant magnetic stirring until the nonformation of turbidity. The vial was closed with a septum and a cap to prevent evaporation and stirred by using a magnetic bar. Each component was added to the vial by using a syringe through the septum. The experimental data were adjusted to the equation proposed by Merchuk et al.[28] (eq 1).

$$[\mathrm{PIL}] = A \times \exp\{(B \times [\mathrm{ACN}]^{0.5}) - (C \times [\mathrm{ACN}]^3)\} \quad (1)$$

where [PIL] and [ACN] are mass fractions of protic ionic liquids and acetonitrile, respectively. *A*, *B*, and *C* are constants obtained by regression of the experimental data.

The tie lines (TL) were determined from compositions in the biphasic region for each system, weighing each component's known mass and adding it to glass tubes with a stopper. The mixtures contained in the tubes were vigorously stirred and centrifuged at 4000 rpm for 5 min for separation and then brought to rest for 24 h at a controlled temperature with an uncertainty of ±0.1 K, allowing equilibrium to be reached and phase separation to be achieved. After equilibration, the top and bottom phases were weighed separately. The phases were removed by using a syringe. The TL determination was then accomplished by solving the following system of four eqs 2−5, as proposed by Merchuk et al.[28]

$$[\mathrm{PIL}]_\mathrm{T} = A \times \exp\{(B \times [\mathrm{ACN}]_\mathrm{T}^{0.5}) - (C \times [\mathrm{ACN}]_\mathrm{T}^3)\} \quad (2)$$

$$[\mathrm{PIL}]_\mathrm{B} = A \times \exp\{(B \times [\mathrm{ACN}]_\mathrm{B}^{0.5}) - (C \times [\mathrm{ACN}]_\mathrm{B}^3)\} \quad (3)$$

https://doi.org/10.1021/acs.iecr.4c03157
Ind. Eng. Chem. Res. 2025, 64, 5602−5616

$$[\mathrm{PIL}]_{\mathrm{T}} = \left(\frac{[\mathrm{PIL}]_{\mathrm{M}}}{\alpha}\right) - \left(\frac{1-\alpha}{\alpha}\right) \times [\mathrm{PIL}]_{\mathrm{B}} \quad (4)$$

$$[\mathrm{ACN}]_{\mathrm{T}} = \left(\frac{[\mathrm{ACN}]_{\mathrm{M}}}{\alpha}\right) - \left(\frac{1-\alpha}{\alpha}\right) \times [\mathrm{ACN}]_{\mathrm{B}} \quad (5)$$

where the subscripts M, T, and B correspond to the mixture point and the top and bottom phases, respectively. The value of α is the ratio of the top phase's mass to the mixture's total mass.

The tie-line length (TLL) was determined by using eq 6. The accuracy of the TLL was determined by comparing the slopes for the different mixing points (tie-line slope, TLS) (eq 7), which must have similar values, demonstrating the parallelism between them.

$$\mathrm{TLL} = \sqrt{([\mathrm{ACN}]_{\mathrm{T}} - [\mathrm{ACN}]_{\mathrm{B}})^2 + ([\mathrm{PIL}]_{\mathrm{T}} - [\mathrm{PIL}]_{\mathrm{B}})^2} \quad (6)$$

$$\mathrm{TLS} = \frac{([\mathrm{ACN}]_{\mathrm{T}} - [\mathrm{ACN}]_{\mathrm{B}})}{([\mathrm{PIL}]_{\mathrm{T}} - [\mathrm{PIL}]_{\mathrm{B}})} \quad (7)$$

2.4. Thermodynamic Modeling. Liquid−liquid equilibrium data for water + PIL + acetonitrile systems were correlated with NRTL and UNIQUAC. The required interaction parameters (A_{ij}, A_{ji}, B_{ij}, B_{ji}, a_{ij}) were calculated using regression in a Fortran routine named TML-LLE.[29] The procedure is based on the modified simplex method using regression and minimization of an objective function, as shown in eq 8

$$S = \sum_{j}^{M} \sum_{i}^{N-1} [(x_{ijk}^{\mathrm{T,exp}} - x_{ijk}^{\mathrm{T,cal}})^2 + (x_{ijk}^{\mathrm{B,exp}} - x_{ijk}^{\mathrm{B,cal}})^2] \quad (8)$$

where M and N are the numbers of components and tie lines in the data set k; superscripts T and B refer to the top and bottom phases in equilibrium, respectively; exp and cal correspond to experimental and calculated data, respectively; and x is the molar fraction.

Structural parameters r and q for ILs were calculated using eqs 9 and 10, as proposed by Santiago et al.[30] Volume and area were generated through quantum calculations using density functional theory (GGA VWN-BP)[31] using Materials Studio software.

$$r = \frac{V \times N_{\mathrm{A}}}{V_{\mathrm{VW}}} \quad (9)$$

$$q = \frac{A \times N_{\mathrm{A}}}{A_{\mathrm{VW}}} \quad (10)$$

where V and A are volume and area, respectively, calculated after minimizing energy for optimizing geometry, and N_{A} is Avogadro's number. V_{VW} and A_{VW} are the van der Waals volume and area of a methylene segment equal to 15.17 $\mathrm{cm^3\ mol^{-1}}$ and $2.5 \times 10^9\ \mathrm{cm^2\ mol^{-1}}$, respectively.

The root-mean-square deviation (RMSD) (eq 11) was used for a comparison between the experimental and calculated data.

$$\mathrm{RMSD} = 100 \sqrt{\frac{\sum_{j}^{M} \sum_{i}^{N-1} [(x_{ijk}^{\mathrm{T,exp}} - x_{ijk}^{\mathrm{T,cal}})^2 + (x_{ijk}^{\mathrm{B,exp}} - x_{ijk}^{\mathrm{B,cal}})^2]}{2MN}} \quad (11)$$

2.5. Target Biomolecules Partitioning. Different ATPSs based on PILs + ACN + water were used to investigate the partitioning of commercial biomolecules in clove oil, such as eugenol, eugenyl acetate, and α-humulene. Three mixing points were performed (A, 15 wt % PIL + 47 wt % ACN + 38 wt % water; B, 15 wt % PIL + 42 wt % ACN + 43 wt % water; and C, 15 wt % PIL + 38 wt % ACN + 47 wt % water) at different temperatures. The systems were prepared in tubes (15 mL), in which the target biomolecule was separately dissolved in ACN to have a final concentration of 45 mg $\mathrm{L^{-1}}$ eugenol, 35 mg $\mathrm{L^{-1}}$ eugenyl acetate, and 8 mg $\mathrm{L^{-1}}$ α-humulene in the system. Afterward, the appropriate amounts of PIL and water were added. Each tube was carefully closed to prevent evaporation of acetonitrile, manually homogenized, and centrifuged at 2000 rpm for 10 min, followed by an equilibrium in a thermostatic bath (ABC Labor, São Bernardo do Campo-SP, Brazil) at different temperatures during at least 24 h. The bottom phase was first separated using a syringe with a long needle, followed by harvesting the top phase using a glass pipette. The volumes and concentrations of target biomolecules in each corresponding phase were measured for all ATPS. Three independent experimental assays were carried out, with the results presented as the average of three independent measurements with associated standard deviations.

The concentrations of each biomolecule in the coexistent phases were determined through ultraviolet (UV) spectroscopy (Shimadzu UV-3600 Plus, Kyoto, Japan) at wavelengths of 279 nm (eugenol), 272 nm (eugenyl acetate), and 203 nm (α-humulene). The calibration curves (Figure S1, Supporting Information) were determined using each standard biomolecule at different concentrations as a blank solution of either water (calibration curve) or the corresponding phase being analyzed (partitioning process). The final absorbance result is reported as the average of three independent findings.

The partition coefficients (K) were determined for each investigated system through the ratio between the concentration of biomolecule in the top (C_{T}) and bottom phase (C_{B}), as described in eq 12.

$$K = \frac{C_{\mathrm{T}}}{C_{\mathrm{B}}} \quad (12)$$

The recovery percentage in the bottom phase (R_{B}) was calculated according to eq 13.

$$R_{\mathrm{B}} = \frac{100}{1 + R_{\mathrm{V}} \times K} \quad (13)$$

where R_{V} is the ratio between the top (V_{T}) and the bottom (V_{B}) volume of the phase. The volumes of the phases depicted in eq 13 were determined more precisely using the mass of each phase and the density measured in an Anton Paar DSA 5000 M analyzer, accurate to 0.005 kg $\mathrm{m^{-3}}$.

The selectivity of the biomolecule (S) was calculated by using the ratio between the partition coefficients of two different target biomolecules and used to evaluate the separation performance of the biomolecules from each other (eq 14).

https://doi.org/10.1021/acs.iecr.4c03157
Ind. Eng. Chem. Res. 2025, 64, 5602−5616

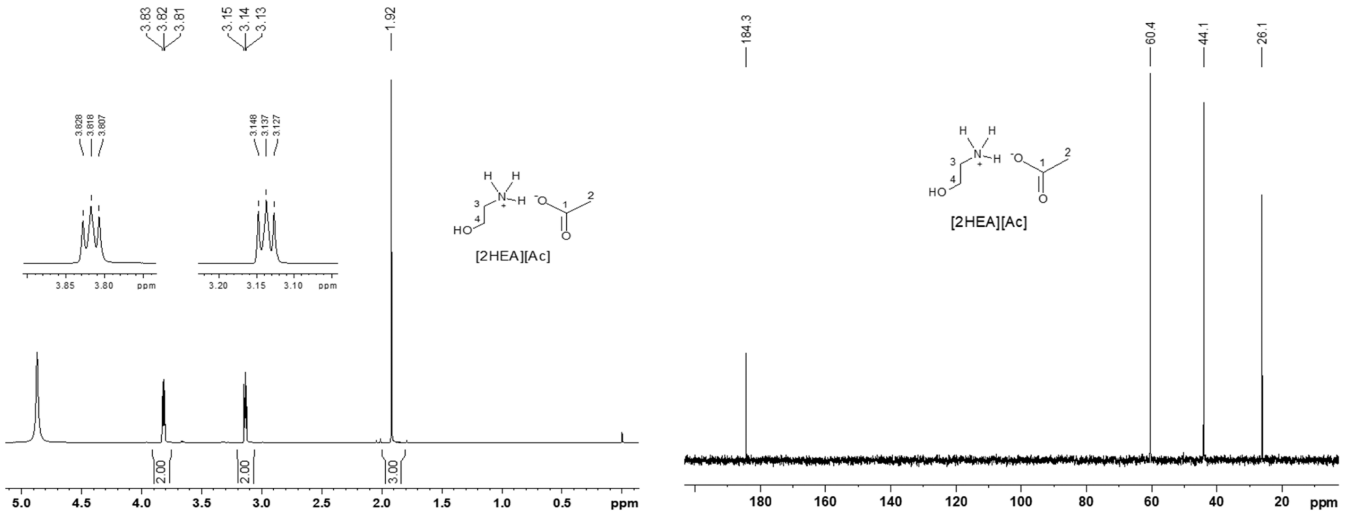

Figure 2. ^{1}H NMR (500 MHz; D_2O) (a) and ^{13}C NMR (125 MHz; D_2O) (b) spectra for [2HEA][Ac].

$$S = \frac{K_i}{K_j} \tag{14}$$

where subscripts i and j represent two different biomolecules.

2.6. Computational Analysis. Sigma profiles were depicted using JCOSMO.[32] The geometry optimization of ATPS constituents and target biomolecules was performed using the continuum solvation COSMO model with semi-empirical quantum calculations through MOPAC/AM1.[33] After optimization, the screening charge distributions on the molecular surface (σ-profile) were calculated.

3. RESULTS AND DISCUSSION

3.1. Protic Ionic Liquid Characterization. The studied PILs in the present paper were characterized by ^{1}H and ^{13}C NMR analyses, whose NMR spectra of the synthesized liquids are shown in Figure 2 for [2HEA][Ac] to illustrate the analysis and the other one in Figures S2−S4 of Supporting Information. For all of the ionic liquids investigated, the 2-hydroxyethylammonium group was characterized by two methylene groups presenting triplet signals at δ 3.14 and δ 3.82 due to the attachment to the N and O atoms, respectively.

The methyl group in all structures confirmed the acetate group at δ 1.92 (*s*, H-2) in ^{1}H NMR spectra. In the same way, the propanoate group was confirmed by the methyl group at δ 1.06 (*t*, H-3) and the methylene group at δ 2.18 (*q*, H-2). The butanoate group was confirmed by the methyl group at δ 0.90 (*t*, H-4) and two methylene groups at δ 1.56 (sex, H-3) and 2.16 (*t*, H-2). The last presents the typical chemical shift of α carboxyl hydrogens. Similar results for [2HEA][Bu] were determined by Alcantara et al.[34] The methyl group confirmed the pentanoate group at δ 0.89 (*t*, H-5) and three methylene groups at δ 1.30 (*sex*, H-4), δ 1.53 (*qui*, H-3), and δ 2.18 (*t*, H-2). The last one has the typical chemical shift of α carboxyl hydrogens. The ^{13}C NMR spectra also presented signals close to δ 185 for carboxyl carbons from ester groups and close to δ 60 for the carbinolic carbons of the 2-hydroxyethylammonium groups.

The signal areas indicated that the samples contain equimolar amounts of the cation and anion constituents of the ionic liquid intended in the synthesis. In addition to the signals of water and ionic liquids, no other important signal was observed, reinforcing the synthesis's success. All of the samples presented an ionic liquid content equal to or greater than 98.0% on a dried basis (Table S1, Supporting Information). The water content of the IL after the synthesis and rotary evaporation steps is reported in Table S1. The values determined for the water content, in mass fraction, were consistently lower than 0.63%.

3.2. Phase Diagram. The effect of temperature (288.2, 298.2, and 308.2 ± 1 K) and the alkyl chain size of PIL anion ([2HEA][Ac], [2HEA][Pr], [2HEA][Bu], and [2HEA][Pe]) with a common cation (2-hydroxyethylamonium—[2HEA]) were evaluated for systems based on PIL + ACN + water at atmospheric pressure (101.2 kPa ± 0.1 kPa). The experimental binodal data for all ATPS systems are shown in Tables S2−S5.

Initially, the influence of temperature was studied on the phase diagram, which is a complex phenomenon of different interactions among the system constituents.[35] Increasing the temperature compressed the biphasic region of the phase diagram, as illustrated in Figure 3. According to Zafarani-Mottar and Hamzehzadeh,[36] the solubility of IL decreasing or the phase-forming ability for a system based on [C_4mim]Br and tripotassium citrate with temperature increasing is responsible for the reduction of biphasic area, as observed in this work. At the same time, Han et al.[37] attributed the observation to the instability of the hydration layer around the ionic liquid. This behavior indicates an endothermic character of the phase separation process.[38] On the other hand, traditional ATPSs based on polymers and salt have no significant effect using temperatures below 312.2 K, as observed by Silva et al.[39] using triblock copolymer and salts.

The effect of the ionic liquid on phase separation was attributed to the anion since all protic ionic liquids share the same cation (2-hydroxyethylammonium)—$[2HEA]^+$. The increase in the alkyl chain, and consequently, the hydrophobicity based on the logarithm of the octanol−water coefficient ($\log K_{ow}$) decreases the phase separation in the order [2HEA][Ac] (−3.00) > [2HEA][Pr] (−2.52) > [2HEA][Bu] (−1.53) > [2HEA][Pe] (−0.99), as shown Figure 4. PILs act as a salting-out agent, and as ACN has more hydrophobic characteristics than PILs ($\log K_{ow}$ = −0.17), more

https://doi.org/10.1021/acs.iecr.4c03157
Ind. Eng. Chem. Res. 2025, 64, 5602−5616

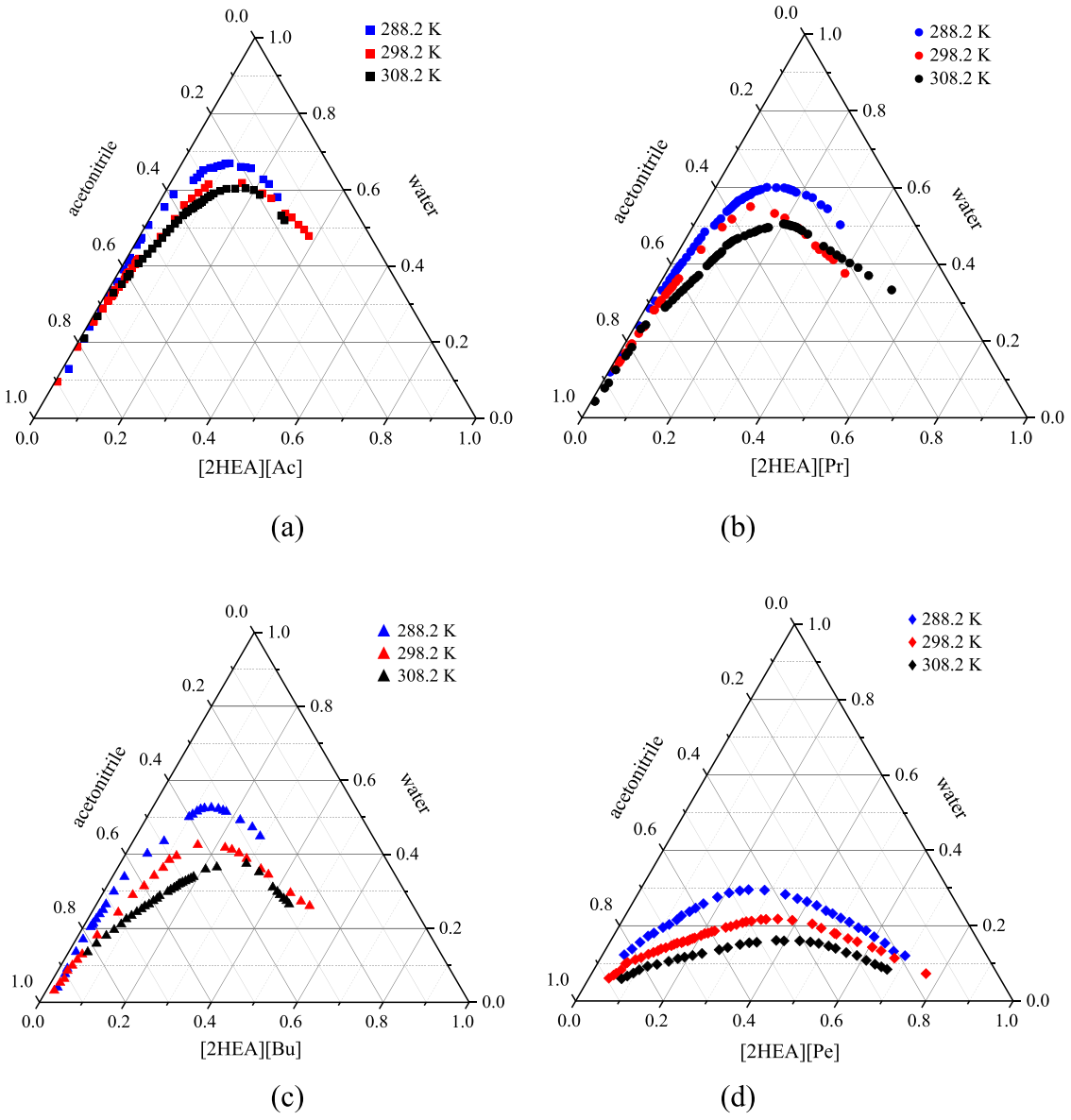

Figure 3. Phase diagrams for PIL ([2HEA][Ac], [2HEA][Pr], [2HEA][Bu], and [2HEA][Pe]) + water + ACN in mass fraction at different temperatures.

hydrophilic PILs separate the phases more easily. This observation corroborates the results of Placido et al.[11] Moreover, the increase in the alkyl chain of the anion increases the solubility of PIL in organic solvent, making phase separation difficult.[40]

All binodal curves were fitted by the correlation of Merchuk et al.,[28] and the regression of the minimum square estimated the regression parameter and coefficient of determination (R^2), and the standard deviations (σ) were also determined, as shown in Table 2. Three TLs were determined to complete the phase diagram; the composition of the TL, their TLL, constituent composition, and TLS are presented in Tables S6−S9 in the Supporting Information.

R^2 values are between 0.9827 and 0.9988, indicating a good fitting of the experimental data, and $\sigma < 0.0136$, demonstrating a low deviation from the experimental and calculated values. The composition equilibrium data confirmed the water content in the bottom phase is higher than in the top phase. For the same system and temperature, it is observed that the TLSs are similar, indicating that the TLSs are parallel and, therefore, well determined.

To compare the binodal curves between this work and those published by Plácido et al.,[11] the systems based on [2HEA]-[Bu] at 298.2 K were randomly chosen. The binodal curves are pretty similar, and TLS values are practically constant, denoting the accuracy of the determinations (Figure S5). Binodal curves and experimental equilibrium data fitted by eq 1 for the systems (PIL + acetonitrile + water) are shown in the Supporting Information (Figures S6−S9).

3.3. Dissociation of the IL Ions. In this work, ionic liquids were considered as a pseudocomponent, including the cation and the anion, and their dissociation products (amine and acid) were not considered present in the phases, as determining this degree of dissociation is not straightforward. As the ionic liquids are formed from weak acids, the question of how to evaluate the degree of dissociation that the ionic liquid has, or if the acid or the amine should also be considered as a system component, arises. In order to investigate if the

https://doi.org/10.1021/acs.iecr.4c03157
Ind. Eng. Chem. Res. 2025, 64, 5602−5616

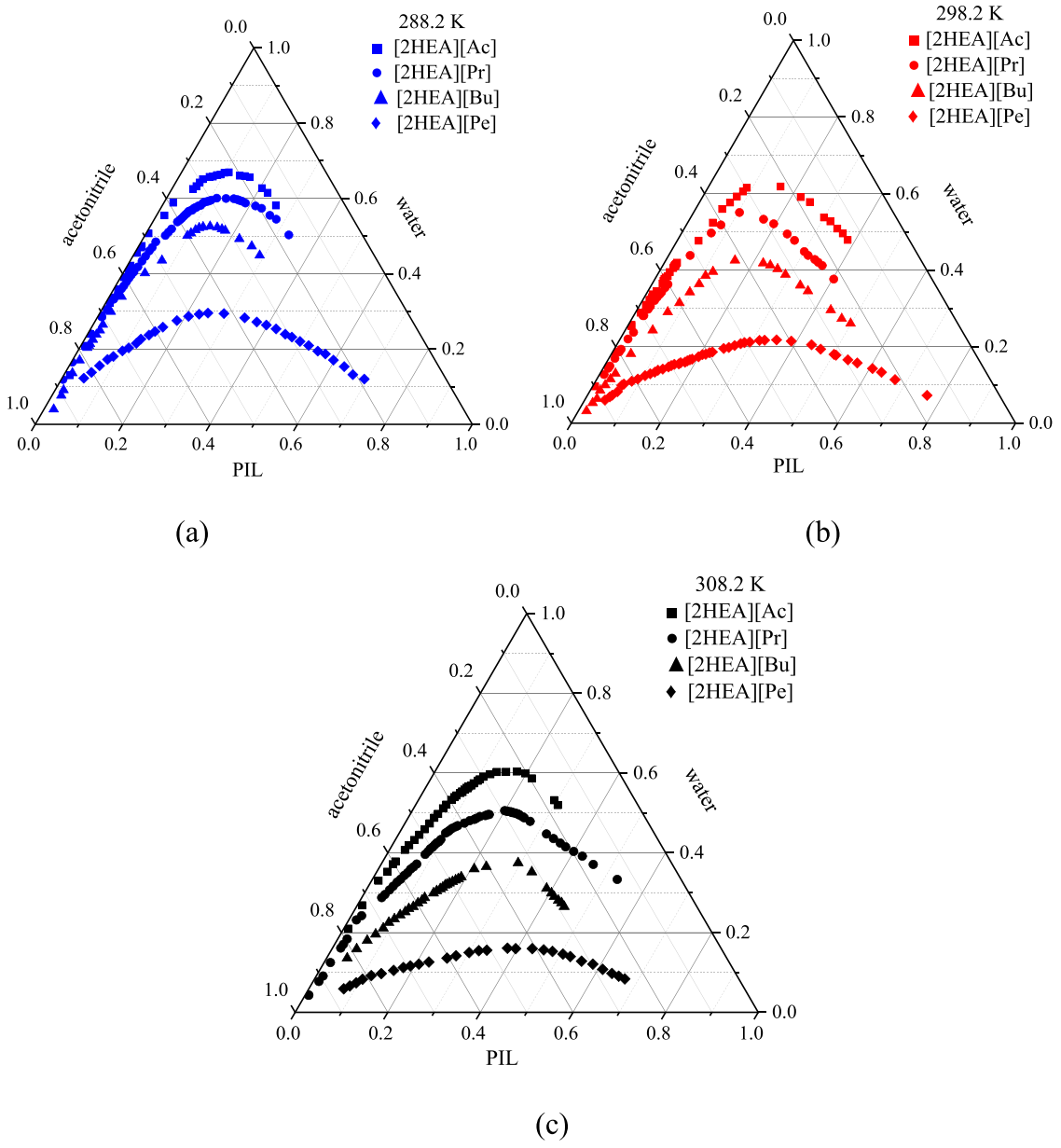

Figure 4. Phase diagrams for PIL + ACN + water in mass fraction at different temperatures.

pseudocomponent hypothesis is reasonable and how to test if it was possible to determine the difference between the ions and their dissociation products, we enriched a [2HEA][Bu] sample with their reagents in unreacted forms, butanoic acid, or monoethanolamine in separate tests, and ^{1}H NMR signals from these reagents were indistinguishable from the respective ionic liquid counterions. On the other hand, an amount of the ionic liquid was put in contact with deuterated oxide + deuterated acetonitrile; the phases were separated, and the spectra of each phase were recorded. We noticed that the counterion ratio maintained the stoichiometry of the ionic liquid after the partition process in the aqueous phase (Figure 5, bottom), while in the acetonitrile fraction (Figure 5, top), the amount of 2HEA decreased by around 20%. Future investigation is warranted to better understand this decrease in the acetonitrile phase. However, the fact that the anion and cation from the ionic liquids were equally partitioned in the aqueous phase supports the hypothesis that they exist as a compound rather than merely a mixture of reagents. Similar results were reported by Buarque et al.,[12] who used FTIR and demonstrated that both salts partition equally in the two phases in an aqueous biphasic system with double protic ionic liquids; therefore, the system could be considered a pseudoternary system.

The phase formation was then tested using only the amine or the corresponding acid. A single phase was formed for any proportion of the components in the systems for all tested mixtures containing amine (2-hydroxyethylamine) + water + acetonitrile and acids (acetic, propanoic, butanoic, and pentanoic) + water + acetonitrile. This indicated that the ionic liquid (cation + anion) is the salting-out agent forming two phases in the acetonitrile−water system.

3.4. Liquid−Liquid Equilibrium Modeling. The experimental data of tie lines were correlated through the thermodynamic models NRTL and UNIQUAC. Each model's binary interaction parameters were estimated and arranged in

https://doi.org/10.1021/acs.iecr.4c03157
Ind. Eng. Chem. Res. 2025, 64, 5602−5616

Table 2. Correlations Parameters of Merchuk Equation to Describe the Experimental Binodal Data for the System PIL + ACN + Water at 288.2, 298.2, and 308.2 K and 0.1 MPa[a], Correlation Coefficients (R^2), and Standard Deviation (σ)[b]

	parameters				
	288.15 K				
PIL	A	B	C	R^2	σ
[2HEA][Ac]	16.98 ± 2.70	−10.77 ± 0.38	−3.94 ± 0.92	0.9911	0.0066
[2HEA][Pr]	7.68 ± 0.44	−7.85 ± 0.13	−0.59 ± 0.35	0.9971	0.0040
[2HEA][Bu]	48.70 ± 9.43	−10.19 ± 0.37	−2.59 ± 0.33	0.9940	0.0062
[2HEA][Pe]	3.37 ± 0.14	−3.56 ± 0.09	1.61 ± 0.13	0.9988	0.0072
	298.15 K				
PIL	A	B	C	R^2	σ
[2HEA][Ac]	7.70 ± 0.57	−8.14 ± 0.19	−1.80 ± 0.39	0.9974	0.0056
[2HEA][Pr]	105.5 ± 12.64	−11.92 ± 0.36	−3.28 ± 0.43	0.9968	0.0084
[2HEA][Bu]	18.89 ± 2.34	−7.37 ± 0.24	−0.69 ± 0.26	0.9966	0.0089
[2HEA][Pe]	2.10 ± 0.06	−2.44 ± 0.06	1.84 ± 0.07	0.9984	0.0073
	308.15 K				
PIL	A	B	C	R^2	σ
[2HEA][Ac]	5.14 ± 0.70	−7.00 ± 0.31	−1.13 ± 0.76	0.9827	0.0090
[2HEA][Pr]	4.51 ± 0.28	−5.59 ± 0.14	0.39 ± 0.29	0.9918	0.0110
[2HEA][Bu]	7.42 ± 1.46	−5.35 ± 0.37	−0.09 ± 0.43	0.9869	0.0136
[2HEA][Pe]	2.14 ± 0.09	−2.30 ± 0.08	1.61 ± 0.09	0.9988	0.0067

[a]Expanded uncertainties for 0.98% confidence are $U(T)$ = 1 K and $U(p)$ = 10 kPa. [b]$\sigma = \sqrt{\left(\sum_{i=1}^{N} \frac{(W_3^{cal} - W_3^{exp})^2}{N}\right)}$, where w_3 is the mass fraction of PIL experimental and calculated by eq 1. N represents the number of data points in the binodal curve.

Table 3 (data for the NRTL model with a nonrandomness parameter α = 0.2) and Table 4 (for the UNIQUAC model). Structural parameters related to the volume and area of each component of the system (r and q) used in the UNIQUAC model are shown in the Supporting Information (Table S10).

The experimental and calculated tie lines are shown in Figure 6 for [2HEA][Ac] at different temperatures. The Supporting Information contains the tie lines for other liquids at different temperatures (Figures S10−S12). RMSD values from the NRTL model were smaller for all systems than those obtained from the UNIQUAC model. The RMSD values obtained by the NRTL and UNIQUAC models were lower than 3.0 and 5.3%, respectively. RMSD (eq 11) expressed as (%) for each system is shown in Table S11 in the Supporting Information. The obtained results show both models' ability to correlate the studied systems' liquid−liquid equilibrium data. However, the NRTL model better describes the behavior. Some studies, such as Sosa et al.,[41] demonstrate that the NRTL thermodynamic model can correlate and predict the behavior of data for ATPS satisfactorily. The larger deviation of UNIQUAC is due to the complexity of the model.

3.5. Partitioning of Target Biomolecules. The experimental data of target biomolecules (eugenol, eugenyl acetate, and α-humulene) at 288.2 or 298.2 K and 101.2 kPa are shown in Table S12 of the Supporting Material.

For the temperature of 308.2 K, experimental data of target biomolecules were not carried out because, with increasing temperature, there is a reduction of phase-forming ability for the system due to the solubility of IL decreasing, thus interfering with the separation. Furthermore, the process will include higher energy requirements and operating costs at 308.2 K than at the other studied temperatures.

For all cases, the top phase corresponded to the ACN-rich phase (ACN: $\log K_{ow}$ = −0.17) with more hydrophobic characteristics than the bottom phase or PIL-rich phase (PIL anion: −3.00 < $\log K_{ow}$ < −0.99; anion PIL—2-hydroxyethanolammonium: Log K_{ow} = −3.42). According to Log K_{ow}, the target biomolecules have hydrophobic characteristics of eugenol (2.611), eugenyl acetate (2.521), and α-humulene (4.878). Therefore, they should preferentially migrate to the top phase, as occurs for α-humulene (1.038 < K < 3.176). However, eugenol (0.160 < K < 1.088) and eugenyl acetate (0.550 < K < 1.307) preferentially migrate to the bottom phase. This modification is probably associated with the donation and acceptance of hydrogen bonds, that is, the interactions between the target biomolecules and the systems constituents, about which we found little information in the literature.[42] In this sense, the quantum chemistry approach can predict, through the chemical potentials of each molecule, the thermodynamic properties of the mixture and expressed as a σ-profile, that is, the screening of charges on the surface of the molecules.[43,44]

ATPS constituents and target biomolecules have a nonpolar character since the most prominent peaks are between −0.01 and 0.01 e·Å^{-2} and therefore a weak interaction with water (Figure S13 of the Supporting Material). These compounds also present peaks in the hydrogen bond acceptance region (sigma >0.01), except α-humulene and acetonitrile, indicating the interaction of eugenol and eugenyl acetate with PIL, and consequently with the bottom phase and justifying their preferential migration to PIL-rich phase. Moreover, Plácido et al.[11] identified that aromatic groups of biomolecules, such as the alkaloids caffeine, theobromine, and theophylline, with the alkyl chain of PIL anions, such as the interactions of the rings, were also present in eugenol and eugenyl acetate and PIL.

In most cases, the temperature increase from 288.2 to 298.2 K increased or maintained almost constant recovery of biomolecules in the bottom phase, which can be attributed to the increased solubility of biomolecules in the PIL-rich phase (Figure 7). According to Martins et al.,[45] the molar

https://doi.org/10.1021/acs.iecr.4c03157
Ind. Eng. Chem. Res. 2025, 64, 5602−5616

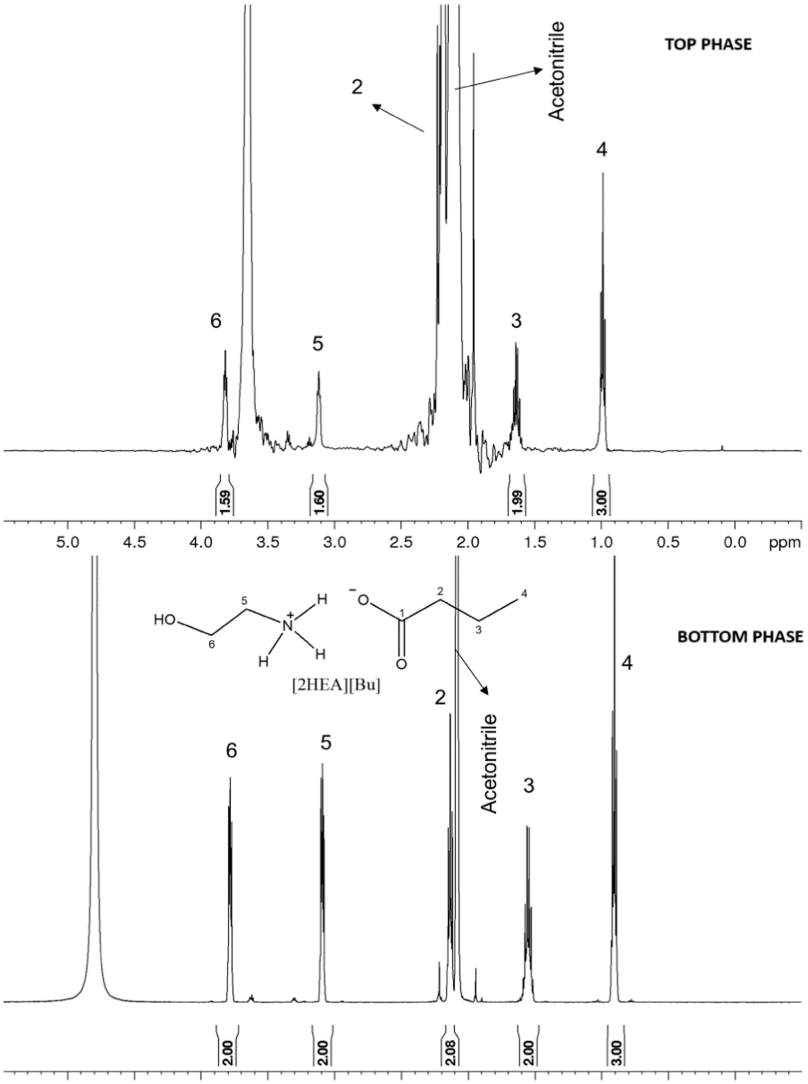

Figure 5. ^{1}H NMR spectrum for [2HEA][Bu] in the top and bottom phase, after partitioning in a mixture of D_2O/CD_3CN (500 MHz, D_2O).

Table 3. NRTL (α_{ij} = 0.20) Parameters Fitted for the System PIL ([2HEA][Ac], [2HEA][Pr], [2HEA][Bu], and [2HEaA][Pe]) + Water + Acetonitrile at 288.2, 298.2, and 308.2 K

$i-j$	A_{ij}/K	A_{ji}/K	B_{ij}/K	B_{ji}/K
[2HEA][Ac]−water	−85,523	2895.4	301.95	−17.493
[2HEA][Ac]−acetonitrile	13,311	11,432	−47.664	−29.739
water−acetonitrile	1957.1	4219.7	−5.5478	−13.481
[2HEA][Pr]−water	6747.7	27.175	−4.7203	−7.5143
[2HEA][Pr]−acetonitrile	−3067.6	8347.1	6.5817	−20.479
[2HEA][Bu]−water	−12281	−7607.8	67.920	19.423
[2HEA][Bu]−acetonitrile	−27,508	2.17×10^5	90.895	−728.12
[2HEA][Pe]−water	−19145	8903	59.812	−32.491
[2HEA][Pe]−acetonitrile	1330.7	−4686.3	−5.1046	17.652

fraction of eugenol in water increases monotonically from 2.28×10^{-4} (298.2 K) to 3.12×10^{-4} (323.2 K). Santos et al.[46] also observed that temperature plays a vital role in the partitioning and recovery of biomolecules because studying the partitioning of biomolecules, the highest migration of caffeine to the alcohol-rich phase was found in systems using potassium salts as a salting-out agent.

Moreover, we studied the behavior of bottom phase recovery of target biomolecules with different PIL anions (alkyl chain sizes from 2 to 5 carbons) at the temperatures studied. It is known that the partition behavior is due to competing interactions (hydrogen bonds, dispersive interactions, and $\pi-\pi$ interactions) between the compounds present in the system.[47] The increase in the alkyl chain size of the PIL anion leads to an increase in hydrophobicity and, consequently, an increase in the recovery of α-humulene in the acetonitrile-rich phase. The α-humulene is a contaminant in the bottom phase, so lower recovery values are preferable

https://doi.org/10.1021/acs.iecr.4c03157
Ind. Eng. Chem. Res. 2025, 64, 5602−5616

Table 4. UNIQUAC Parameters Fitted for the System PIL ([2HEA][Ac], [2HEA][Pr], [2HEA][Bu], and [2HEA][Pe]) + Water + Acetonitrile at 288.2, 298.2, and 308.2 K

$i-j$	A_{ij}/K	A_{ji}/K	B_{ij}/K	B_{ji}/K
[2HEA][Ac]−water	−5259.0	−715.12	18.313	0.27761
[2HEA][Ac]−acetonitrile	−556.98	252.02	0.0021	1.5742
water−acetonitrile	−5933.7	93.885	23.827	−1.7201
[2HEA][Pr]−water	−5137.5	−654.02	20.380	0.28551
[2HEA][Pr]−acetonitrile	−470.37	440.41	0.0184	1.2260
[2HEA][Bu]−water	−361.55	−1796.6	7.2152	4.2690
[2HEA][Bu]−acetonitrile	−613.63	2607.3	0.0326	−4.4011
[2HEA][Pe]−water	1667.0	594.62	−3.7024	7.8022
[2HEA][Pe]−acetonitrile	−227.83	2329.3	−0.5710	−4.5585

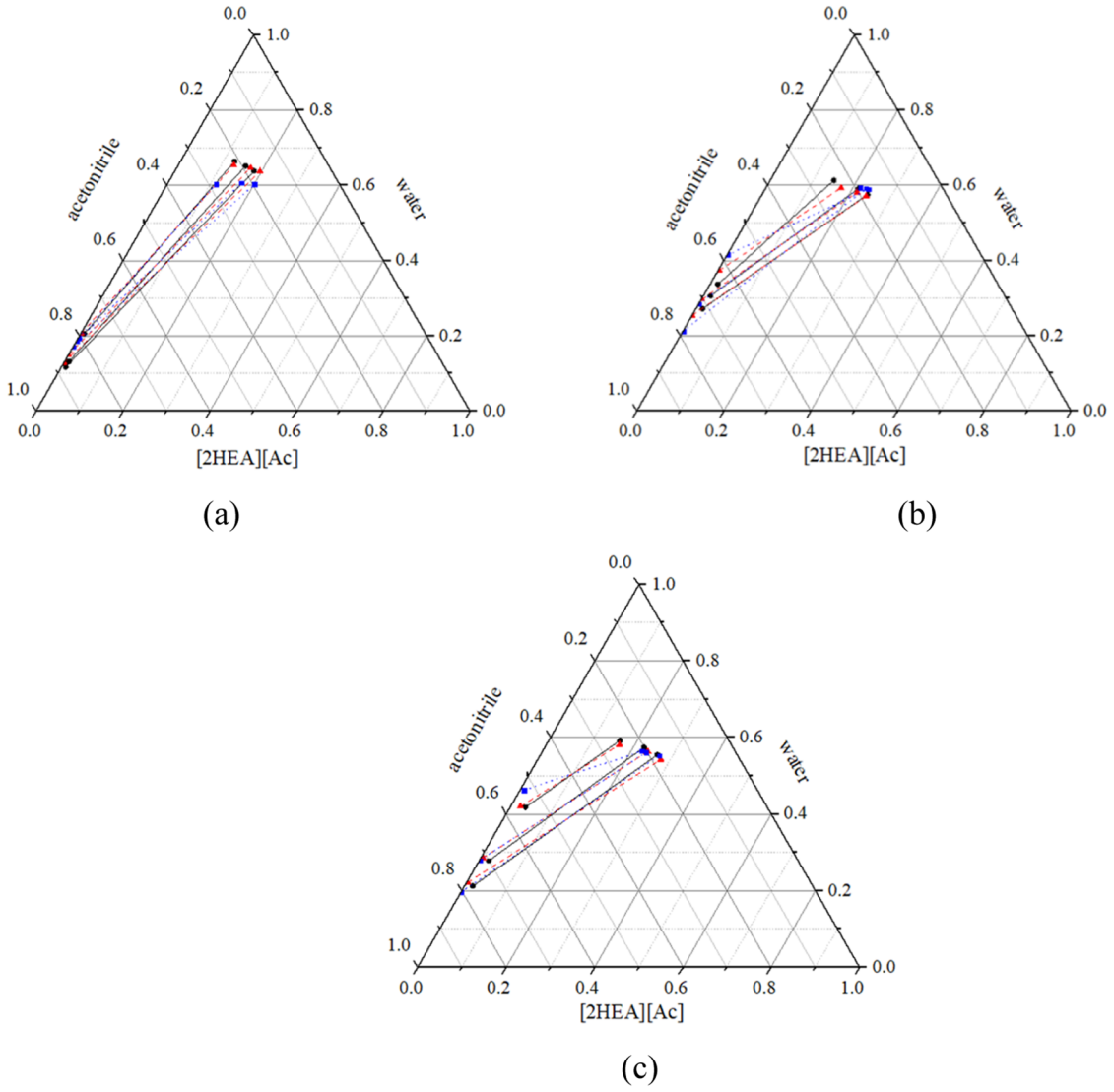

Figure 6. Liquid−liquid equilibrium data for the system [2HEA][Ac] + water + acetonitrile, in mass fraction at 288.2 K (a), 298.2 K, (b) and 308.2 K (c). ●—black solid lines (experimental); (▲, red dashed lines) (NRTL); and, (■, bule dot lines) (UNIQUAC).

because the goal is to understand the behavior of each biomolecule in the system phases to assist in the deterpenation. However, eugenol and eugenyl acetate have their bottom phase recovery reduced from acetate to propanoate, from which the systems formed by butanoate and pentanoate have a background recovery similar to that of the shorter alkyl chain. This result is probably due to the hydrophilic−hydrophobic balance between the cations and anions of PILs.

The highest values achieved for bottom phase recoveries for the target biomolecules were achieved using [2HEA][Bu]. Dias et al.[40] studied the partitioning of lignin in systems formed by PILs + acetone + water and observed that the increase in the alkyl chain could favor interactions between PILs and target biomolecules, increasing migration to the bottom phase, to the detriment of the characteristic hydrophobicity of these molecules. This trend was also observed in

https://doi.org/10.1021/acs.iecr.4c03157
Ind. Eng. Chem. Res. 2025, 64, 5602−5616

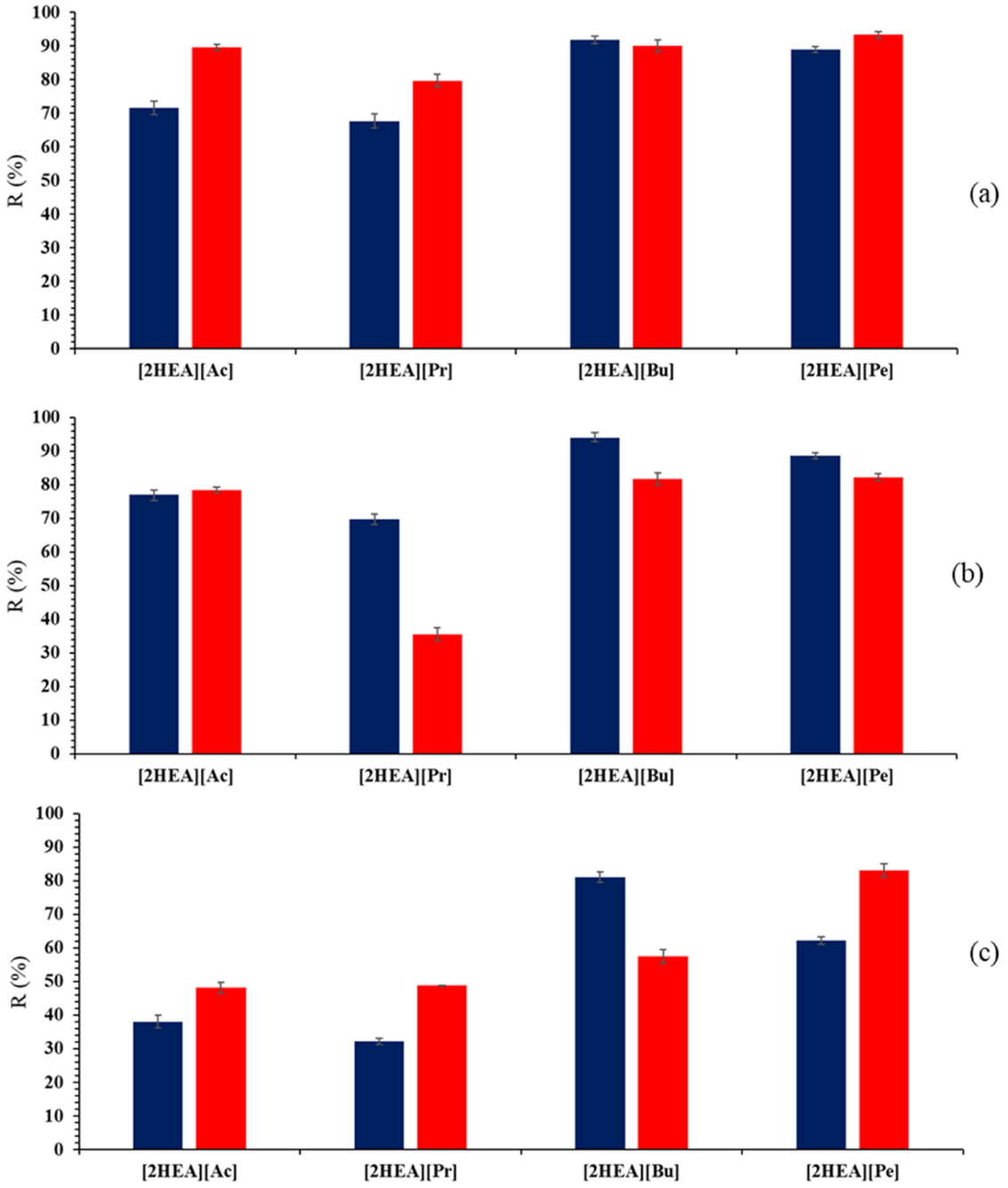

Figure 7. Effect of temperature (blue box solid, 288.2 K; brown box solid, 298.2 K) on the biomolecule recovery in the bottom phase (a, eugenol; b, eugenyl acetate; c, α-humulene) using an aqueous two-phase system formed by protic ionic liquids ([2HEA][Ac]: TLL ≈ 58; [2HEA][Pr]: TLL ≈ 52; [2HEA][Bu]: TLL ≈ 53, and [2HEA][Pe]: TLL ≈ 53) + acetonitrile and water at 101.2 kPa.

this study for the eugenol and eugenyl acetate molecules, corroborating the results presented.

Figure 8 depicts the selectivity results of all target biomolecules on the ATPS based on [2HEA][Bu] + ACN + water due to the best recovery in the bottom phase. Increasing the temperature allows for better separation of biomolecules. It is still possible to observe that α-humulene can be easily separated ($2.93 < S < 6.83$) from eugenol and eugenyl acetate in both studied temperatures. Additionally, eugenol and eugenyl acetate can be partially isolated ($S = 2.17$) at 298.2 K. Buarque et al.[12] also reported the possibility of selective separation of compounds such as hormones in PIL-based ATPS.

To illustrate the enrichment of the target biomolecules studied here in one of the phases, we present a conceptual process diagram formed by different steps (Figure 9): (a) extraction of clove oil containing eugenol, eugenyl acetate, and α-humulene using acetonitrile; (b) separation of target biomolecules using the systems presented in this work; and (c) recycling and reuse of the phases formed using antisolvent as an alternative to enhance the sustainable character of the process. Acetonitrile, present as the majority constituent of the top phase, has a boiling point of 82 °C. In contrast, α-humulene, a biomolecule that preferentially migrates to the ACN-rich phase, has a boiling point of 106 °C. Therefore, the target biomolecule can be separated, and the ACN can be

https://doi.org/10.1021/acs.iecr.4c03157
Ind. Eng. Chem. Res. 2025, 64, 5602−5616

288.2K

		EUG	EAC	HUM
	K	0.527	0.422	1.542
EUG	0.527	1.00	0.80	2.93
EAC	0.422	1.2	1.00	3.65
HUM	1.542	0.34	0.27	1.00

Selectivity Values	
S < 1.0	
S = 1.0	
1.0 > S > 3.0	
S ≥ 3.0	

298.2 K

		EUG	EAC	HUM
	K	0.190	0.413	1.298
EUG	0.190	1.00	2.17	6.83
EAC	0.413	0.46	1.00	3.14
HUM	1.298	0.15	0.32	1.00

Figure 8. Selectivity of target biomolecules present in clove oil (eugenol, EUG; eugenyl acetate, EAC; and α-humulene, HUM) using an aqueous two-phase system based on [2HEA][Bu] + ACN + water at different temperatures.

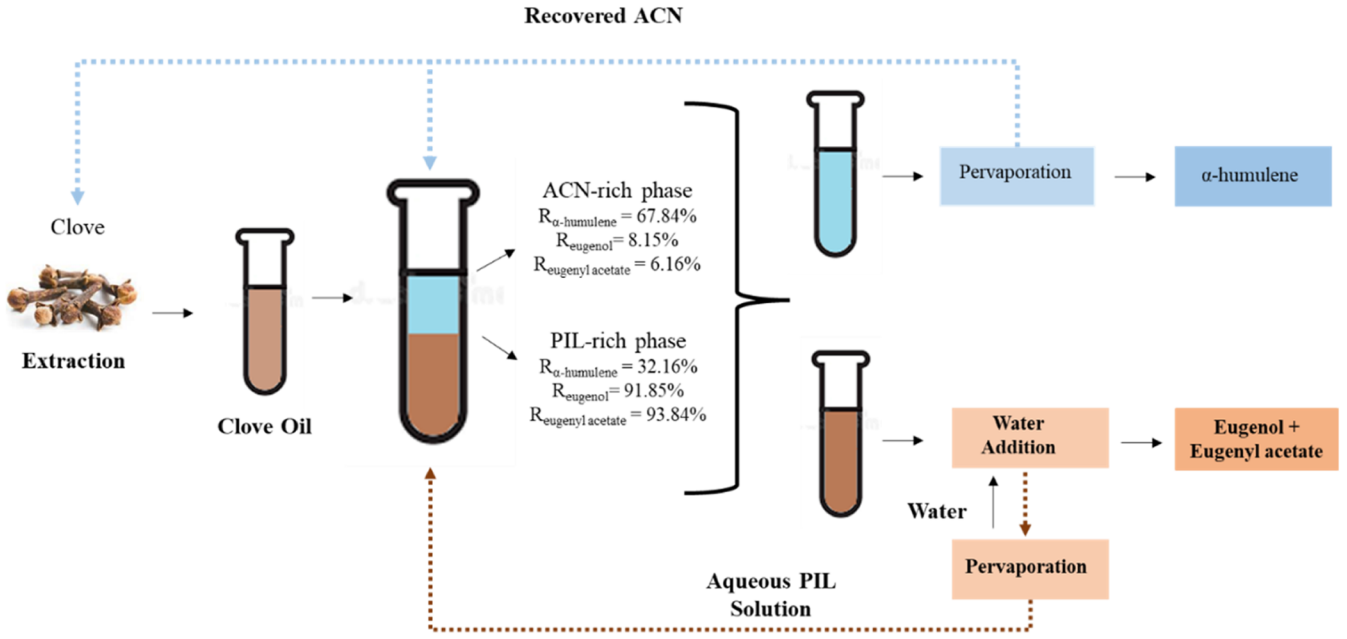

Figure 9. Conceptual flowchart of isolating active biomolecules from clove oil using an aqueous two-phase system based on [2HEA][Bu] + ACN + water at 298.2 K and atmospheric pressure.

recycled for the extraction process or the composition of new systems. Eugenol and eugenyl acetate are insoluble in water. Therefore, they can be separated by adding water as an antisolvent and forming two liquid phases. This way, the excess water added can be distilled to return to the system, and the aqueous PIL solution can be reused to replenish the ATPS.

4. CONCLUSIONS

Liquid−liquid equilibrium data for the ternary systems PIL + acetonitrile + water at 288.2, 298.2, and 308.2 K were obtained experimentally. The experimental binodal data were obtained satisfactorily to study ionic liquids' behavior as salting-out components in the acetonitrile−water mixture. The effects of temperature and the alkyl chain size of the PIL anion were observed in the behavior of the phase diagram. Thus, the increase in the alkyl chain decreases the phase separation in the order [2HEA][Ac] > [2HEA][Pr] > [2HEA][Bu] > [2HEA]-[Pe] and decreases as the temperature increases. The phenomena reported in this work are considered to be analyzed by Log K_{ow} and by the interaction between the PIL-water and water-ACN. The PIL studies showed greater affinity for the water-rich phase, demonstrating a hydrophilic character at all temperatures investigated. The NRTL and UNIQUAC models correlated the experimental data. The results indicate that the NRTL and UNIQUAC models can be used for the prediction of LLE data for the PIL + acetonitrile + water system, presenting root-mean-square deviations (RMSD) always lower than 3.0 and 5.3%, respectively, considering each separate and global system. However, the NRTL model better describes the behavior.

The partition of the biomolecules was studied at 288.2 and 298.2 K, and the results indicated that eugenol and eugenyl acetate preferred the bottom phase or PIL-rich phase and that α-humulene migrated to the top phase or ACN-rich phase. The study also sought to understand, through computational analysis, the polar character of the system constituents to evaluate possible interactions. The temperature increase from 288.2 to 298.2 K increased the recovery of biomolecules in the bottom phase, mainly for phenolics (eugenol and eugenyl acetate). The system formed with [2HEA][Bu] showed greater

https://doi.org/10.1021/acs.iecr.4c03157
Ind. Eng. Chem. Res. 2025, 64, 5602−5616

selectivity for separating target biomolecules. It was also possible to observe that α-humulene can be easily separated from eugenol and eugenyl acetate in both studied temperatures ($S > 1$), assisting in deterpenation. Therefore, the presented results can be used for the isolation and purification of the commercial biomolecules present in clove oil.

■ ASSOCIATED CONTENT

Supporting Information

The Supporting Information is available free of charge at https://pubs.acs.org/doi/10.1021/acs.iecr.4c03157.

^{1}H and ^{13}C spectra of the purified PILs (Figures S1−S3); binodal curve adjusted (Figures S4−S8); equilibrium data (Figures S9−S11); representation of σ-profiles (Figure S12); purity and water content of the PILs (Table S1); experimental binodal curve data (Table S2−S5); phase composition, TLL, and TLS (Tables S6−S9); UNIQUAC parameters (Table S10); RMSD of NTRL and UNIQUAC (Table S11); and partition and recovery of biomolecules (Table S12) (PDF)

■ AUTHOR INFORMATION

Corresponding Author

Silvana Mattedi − *Chemical Engineering Graduate Program, Polytechnic School, Federal University of Bahia (UFBA), Salvador, Bahia 40210-630, Brazil;* orcid.org/0000-0003-4816-7494; Email: silvana@ufba.br

Authors

Jarlon Conceição da Costa − *Chemical Engineering Graduate Program, Polytechnic School, Federal University of Bahia (UFBA), Salvador, Bahia 40210-630, Brazil*

Isabela Conceição Sales − *Chemical Engineering Graduate Program, Polytechnic School, Federal University of Bahia (UFBA), Salvador, Bahia 40210-630, Brazil;* orcid.org/0000-0002-8048-1072

Bruna Vida da Ressureição − *Chemical Engineering Graduate Program, Polytechnic School, Federal University of Bahia (UFBA), Salvador, Bahia 40210-630, Brazil*

Luciano Morais Lião − *Federal University of Goiás (UFG), Institute of Chemistry, Goiânia, Goiás 74690-900, Brazil;* orcid.org/0000-0001-9985-2980

Gerlon de Almeida Ribeiro Oliveira − *Pharmacy Department, Health Sciences Faculty, University of Brasília (UnB), Brasília, Federal District 70910-900, Brazil*

Álvaro Silva Lima − *Chemical Engineering Graduate Program, Polytechnic School, Federal University of Bahia (UFBA), Salvador, Bahia 40210-630, Brazil*

Luiz Mário N Góis − *Chemical Engineering Graduate Program, Polytechnic School, Federal University of Bahia (UFBA), Salvador, Bahia 40210-630, Brazil; School of Architecture, Engineering and Information Technology, Salvador University, Salvador, Bahia 41770-235, Brazil*

Complete contact information is available at: https://pubs.acs.org/10.1021/acs.iecr.4c03157

Funding

The Article Processing Charge for the publication of this research was funded by the Coordenacao de Aperfeicoamento de Pessoal de Nivel Superior (CAPES), Brazil (ROR identifier: 00x0ma614).

Notes

The authors declare no competing financial interest.

■ ACKNOWLEDGMENTS

The authors are grateful to FAPESB/SECTI/Governo da Bahia/Brazil, CAPES, and CNPq/Brazil for financial support. CAPES is also acknowledged for Web of Science access through the Periodicos website. The authors thank Víctor Álvarez for quantum calculation with Material Studio software.

■ ABBREVIATIONS

ILionic liquid
PILprotic ionic liquid
AILaprotic ionic liquid
ACNacetonitrile
ATPSaqueous two-phase system
[2HEA]2-hidroxylethylammonium
[Ac]acetate
[Pr]propanoate
[Bu]butanoate
[Pe]pentanoate
A, B, and Cconstants obtained by regression
TLtie lines
TLLtie-line length
TLStie-line slope
NRTLnon-random two-liquid
UNIQUACUniversal Quasichemical
A_{ij}, A_{ji}, B_{ij}, B_{ji} *e* a_{ij}interaction parameters
*x*molar fraction
*M*number of components
*N*number of tie lines
RMSDroot-mean-square deviation
*V*volume
*A*area
V_{VW}van der Waals volume
A_{VW}van der Waals area
N_AAvogadro's number
r and *q*structural parameters
*K*partition coefficients
*C*concentration of biomolecule
$R_B$recovery percentage in the bottom phase
*S*selectivity of the biomolecule
^{13}C NMR^{13}C, ^{1}H NMR nuclear magnetic resonance spectroscopy
*w*mass fraction
R^2correlation coefficients
σstandard deviation

■ SUPERSCRIPTS

Ttop phase
Bbottom phase
expexperimental
calcalculated

■ SUBSCRIPTS

Mmixture point
Ttop phase
Bbottom phase
i,*j*chemical species
*k*data set

REFERENCES

(1) Vilas-Boas, S. M.; Coelho, A. Z.; Martins, M. A. R.; Coutinho, J. A. P.; Ferreira, O.; Pinho, S. P. Evaluation of Ionic Liquids for the Sustainable Fractionation of Essential Oils. *Ind. Eng. Chem. Res.* **2023**, *62*, 6749−6758.

(2) Sousa, K. M.; Lima, T. S. P.; Souza, R. L.; Nerli, B. B.; Pereira, M. M.; Soares, C. M. F.; Lima, A. S. Liquid-liquid equilibrium data for the ternary system based on ionic liquid + organic solvents + water at 298 K and atmospheric pressure applied in antidepressant partitioning. *Sep. Purif. Technol.* **2022**, *278*, No. 119532.

(3) da Silva, L. H.; Meirelles, A. J. A. Phase equilibrium and protein partitioning in aqueous mixtures of maltodextrin with polypropylene glycol. *Carbohydr. Polym.* **2001**, *46* (3), 267−274.

(4) Mo, Y. L.; Fischlschweiger, M.; Zeiner, T. Polymeric Aqueous Two Phase System with an Immobilized Phase by Cross-Linking. *Ind. Eng. Chem. Res.* **2022**, *61*, 15381−15389.

(5) Dias, R. M.; Petrin, L. C. G.; Sosa, F. H. B.; Lopes, A. M. C.; Coutinho, J. A. P.; Costa, M. C. Investigation of Kraft Lignin Solubility in Protic Ionic Liquids and Their Aqueous Solutions. *Ind. Eng. Chem. Res.* **2020**, *59*, 18193−18202.

(6) Marchel, M.; João, K. G.; Marrucho, I. M. On the use of ionic liquids as adjuvants in PEG-$(NH_4)_2SO_4$ aqueous biphasic systems: Phase diagrams behavior and the effect of IL concentration on myoglobin partition. *Sep. Purif. Technol.* **2019**, *210*, 710−718.

(7) Haro-Gonzaléz, J. N.; Castillo-Herrera, G. A.; Martínez-Velázquez, M.; Espinosa-Andrews, H. Clove essencial oil (*Syzygium aromaticum* L. Myrtaceae): Extraction, Chemical composition, food applications, and essential bioactivity for Human health. *Molecules* **2021**, *26*, No. 6387.

(8) Wang, L.-H. Fragrances: from essential oils to the human body and atmospheric aerosol. *Anal. Methods* **2013**, *2*, 316−322.

(9) Koshima, C. C.; Umeda, T. K.; Nakamoto, K. T.; Venâncio, L. L.; Aracava, K. K.; Rodrigues, C. E. C. (Liquid + liquid) equilibrium for systems composed of clove and allspice essential oil compounds and hydrous ethanol at T = 298.2 K. *J. Chem. Thermodyn.* **2016**, *95*, 54−62.

(10) DelMastro, T.; Snow, N. H.; Murphy, W. R.; Sowa, J. R. Polyol-induced partitioning of essential oils in water/acetonitrile solvent mixtures. *J. Liq. Chromatogr. Relat. Technol.* **2017**, *40*, 376−383.

(11) Plácido, N. S.; Carlos, A. L. S.; Galvão, J. U. S.; Souza, R. L.; Soares, C. M. F.; Mattedi, S.; Fricks, A. T.; Lima, A. S. Protic ionic liquids as a constituent of biphasic systems based on acetonitrile: Phase diagram and alkaloid partitioning. *Sep. Purif. Technol.* **2018**, *200*, 318−326.

(12) Buarque, F. S.; Barreto, V. S.; Soares, C. M. F.; Souza, R. L.; Pereira, M. M.; Lima, A. S. Selective extraction of female hormones using aqueous two-phase system composed of double protic ionic liquid + acetonitrile. *Fluid Phase Equilib.* **2020**, *508*, No. 112443.

(13) Buarque, F. S.; Gautério, G. V.; Coelho, M. A. Z.; Lemes, A. C.; Ribeiro, B. D. Aqueous Two-Phase Systems Based on Ionic Liquids and Deep Eutectic Solvents as a Tool for the Recovery of Non-Protein Bioactive Compounds - A Review. *Processes* **2023**, *11* (1), No. 31.

(14) Iqbal, M.; Tao, Y.; Xie, S.; Zhu, Y.; Chen, D.; Wang, X.; Huang, L.; Peng, D.; Sattar, A.; Shabbir, M. A. B.; Hussain, H. I.; Ahmed, S.; Yuan, Z. Aqueous two-phase system (ATPS): an overview and advances in its applications. *Biol. Proced. Online* **2016**, *18*, No. 18.

(15) Rogers, R. D.; Seddon, K. R. *Ionic Liquids in Synthesis*; Wasserscheid, P.; Welton, T., Eds.; Wiley- VCH: Weinheim, Germany, 2003.

(16) Sales, I.; Abranches, D. O.; Sintra, T. E.; Mattedi, S.; Freire, M. G.; Coutinho, J. A. P.; Pinho, S. P. Selection of hydrotropes for enhancing the solubility of artemisinin in aqueous solutions. *Fluid Phase Equilib.* **2022**, *562*, No. 113556.

(17) Han, J.; Wang, Y.; Yu, C.; Li, Y.; Kang, W.; Yan, Y. (Liquid + liquid) equilibrium of (imidazolium ionic liquids + organic salts) aqueous two-phase systems at T = 298.15 K and the influence of salts and ionic liquids on the phase separation. *J. Chem. Thermodyn.* **2012**, *45*, 59−67.

(18) Passos, H.; Freire, M. G.; Coutinho, J. A. P. Ionic liquid solutions as extractive solvents for value-added compounds from biomass. *Green Chem.* **2014**, *16*, 4786−4815.

(19) Baaqel, H.; Hallett, J. P.; Guillén-Gosálbez, G.; Chachuat, B. Sustainability Assessment of Alternative Synthesis Routes to Aprotic Ionic Liquids: The Case of 1-Butyl-3-methylimidazolium Tetrafluoroborate for Fuel Desulfurization. *ACS Sustainable Chem. Eng.* **2022**, *10*, 323−331.

(20) Greaves, T. L.; Drummond, C. J. Protic Ionic Liquids: Properties and Applications. *Chem. Rev.* **2008**, *108*, 206−237.

(21) Peric, B.; Sierra, J.; Martí, E.; Cruañas, R.; Garau, M. A.; Arning, J.; Bottin-Weber, U.; Stolte, S. (Eco)Toxicity and biodegradability of selected protic and aprotic ionic liquids. *J. Hazard. Mater.* **2013**, *261*, 99−105.

(22) Passos, H.; Luís, A.; Coutinho, J. A. P.; Freire, M. G. Thermoreversible (Ionic Liquid-Based) Aqueous Biphasic Systems. *Sci. Rep.* **2016**, *6*, No. 20276.

(23) Alashkar, A.; Al-Othman, A.; Tawalbeh, M.; Qasim. A critical review on the use of ionic liquids in proton Exchange membrane fuel cells. *Membranes* **2022**, *12*, No. 178.

(24) Santos, J. H.; Silva, F. A.; Ventura, S. P. M.; Coutinho, J. A. P.; Souza, L. R.; Soares, C. M. F.; Lima, A. S. Ionic liquid-based aqueous biphasic systems as a versatile tool for the recovery of antioxidant compounds. *Biotechnol. Prog.* **2015**, *31*, 70−77.

(25) de Brito Cardoso, G.; Souza, I. N.; Pereira, M. M.; Freire, M. G.; Soares, C. M. F.; Lima, A. S. Aqueous two-phase systems formed by biocompatible and biodegradable polysaccharides and acetonitrile. *Sep. Purif. Technol.* **2014**, *136*, 74−80.

(26) Álvarez, V. H.; Dosil, N.; Gonzalez-Cabaleiro, R.; Mattedi, S.; Martin-Pastor, M.; Iglesias, M.; Navaza, J. M. Brønsted Ionic liquids for sustainable processes: Synthesis and Physical properties. *J. Chem. Eng. Data* **2010**, *55*, 625−632.

(27) Kaul, R. H. *Aqueous Two-Phase Systems, Methods and Protocols*; Humana Press: NJ, 2000.

(28) Merchuk, J. C.; Andrews, B. A.; Asenjo, J. A. Aqueous two-phase systems for protein separation. Studies on phase inversion. *J. Chromatogr. B: Biomed. Sci. Appl.* **1998**, *711*, 285−293.

(29) Stragevitch, L.; D'Ávila, S. G. Application Of A Generalized Maximum Likelihood Method In The Reduction Of Multicomponent Liquid-Liquid Equilibrium Data. *Braz. J. Chem. Eng.* **1997**, *14*, 41−52.

(30) Santiago, R. S.; Santos, G. R.; Aznar, M. UNIQUAC correlation of liquid-liquid equilibrium in systems involving ionic liquids: The DFT−PCM approach. *Fluid Phase Equilib.* **2009**, *278*, 54−61.

(31) Mullins, E.; Oldland, R.; Liu, Y. A.; Wang, S.; Sandler, S. I.; Chen, C. C.; Zwolak, M.; Seavey, K. C. Sigma-Profile Databases for using COSMO-Based Thermodynamic Methods. *Ind. Eng. Chem. Res.* **2006**, *45*, 4389−4415.

(32) Stewart, J. J. P. MOPAC2016, Stewart Computational Chemistry, Colorado Springs CO, USA. http://OpenMOPAC.net.

(33) Ferrarini, F.; Flores, G. B.; Muniz, A. R.; et al. An open and extensible sigma profile database for COSMO-based models. *AIChE J.* **2018**, *64*, 3443−3455.

(34) Alcantara, M. L.; Carvalho, M. L.; Alvarez, V. H.; Ferreira, P. I. S.; Paredes, M. L. L.; Cardozo-Filho, L.; Silva, A. K.; Lião, L. M.; Pires, C. A. M.; Mattedi, S. High-pressure vapor-liquid equilibria for binary carbon dioxide and protic ionic liquid based on ethanolamines + butanoic acid. *Fluid Phase Equilib.* **2018**, *460*, 162−174.

(35) Guo, J.; Xu, S.; Qin, Y.; Li, Y.; Lin, X.; He, C.; Dai, S. The temperature influence on the phase behavior of ionic liquid-based aqueous two-phase systems and its extraction efficiency of 20chlorophenol. *Fluid Phase Equilib.* **2020**, *506*, No. 112394.

(36) Zafarani-Mottar, M. T.; Hamzehzadeh, S. Phase diagram for the aqueous two-phase ternary system containing the ionic liquid 1-butyl-3methylimizdazolium bromide and tri-potassium citrate at T = (278.15, 298.15 and 318.15) K. *J. Chem. Eng. Data* **2009**, *54*, 833−841.

(37) Han, J.; Pan, R.; Xie, X.; Wang, Y.; Yan, Y.; Yin, G.; Guan, W. Liquid-Liquid equilibria of ionic liquid 1-butyl-3-methylimidazolium tetrafluoroborate+sodium and ammonium citrate aqueous two-phase

https://doi.org/10.1021/acs.iecr.4c03157
Ind. Eng. Chem. Res. 2025, 64, 5602−5616

systems at (298.15, 308.15, and 323.15) K. *J. Chem. Eng. Data* **2010**, *55*, 3749−3754.
(38) Murari, G. F.; Penido, J. A.; Machado, P. A. L.; Lemos, L. R.; Lemes, N. H. T.; Virtuoso, L. S.; Rodrigues, G. D.; Mageste, A. B. Phase diagrams of aqueous two-phase systems formed by polyethylene glycol + ammonium sulfate + water: equilibrium data and thermodynamic modelling. *Fluid Phase Equilib.* **2015**, *406*, 61−69.
(39) Silva, L. H. M.; Silva, M. C. H.; Mesquita, A. F.; Nascimento, K. S.; Coimbra, J. S. R.; Minim, L. A. Equilibrium phase behavior of triblock copolymer + salt + water two-phase systems at different temperature and pH. *J. Chem. Eng. Data* **2005**, *50*, 1457−1461.
(40) Dias, R. M.; Netto, G. C. A.; Petrin, L. C. G.; Pelaquim, F. P.; Sosa, F. H. B.; Costa, M. C. Aqueous two-phase system formed by alkanolammonium-based protic ionic liquids and acetone: Experimental data, thermodynamic modeling, and Kraft lignin partition. *Sep. Purif. Technol.* **2020**, *250*, No. 117207.
(41) Sosa, F. H.; Kilpeläinen, I.; Rocha, J.; Coutinho, J. A. P. Recovery of superbase ionic liquid using aqueous two-phase systems. *Fluid Phase Equilib.* **2023**, *573*, No. 113857.
(42) Khan, I.; Taha, M.; Pinho, S. P.; Coutinho, J. A. P.; et al. Interactions of pyridinium or piperidinium based ionic liquid with water: measurements and COSMO-RS modelling. *Fluid Phase Equilib.* **2016**, *414*, 93−100.
(43) Fallanza, M.; Gonzales-Miquel, M.; Ruiz, E.; Ortiz, A.; Gorri, D.; Palomar, J.; Ortiz, I. Screening of RTILs for propane/propylene separation using COSMO-RS methodology. *Chem. Eng. J.* **2013**, *220*, 284−293.
(44) Banerjee, T.; Sahoo, R. K.; Rath, S. S.; Kumar, R.; Khanna, A. Multicomponent liquid-liquid equilibria prediction for aromatic extraction system using COSMO-RS. *Ind. Eng. Chem. Res.* **2007**, *46*, 1292−1304.
(45) Martins, M. A. R.; Silva, L. P.; Ferreira, O.; Schöder, B.; Coutinho, J. A. P.; Pinho, S. P. Terpenes solubility in water and their environmental distribution. *J. Mol. Liq.* **2017**, *241*, 996−1002.
(46) Santos, S. B.; Reis, I. A. O.; Silva, C. P. C.; Campos, A. F.; Ventura, S. P. M.; Soares, C. M. F.; Lima, A. S. Selective partition of caffeine from coffee bean and guaraná seed extracts using alcohol-salt aqueous two-phase systems. *Sep. Sci. Technol.* **2016**, *51*, 2008−2019.
(47) Soares, B.; Tavares, D. J. P.; Amaral, J. L.; Silvestre, A. J. D.; Freire, C. S. R.; Coutinho, J. A. P. Enhanced Solubility of Lignin Monomeric Model Compounds and Technical Lignins in Aqueous Solutions of Deep Eutectic Solvents. *ACS Sustainable Chem. Eng.* **2017**, *5*, 4056−4065.

https://doi.org/10.1021/acs.iecr.4c03157
Ind. Eng. Chem. Res. 2025, 64, 5602−5616